



# Increasing the high rate performance of mixed metal phospho-olivine cathodes through collective and cooperative strategies



Bo Ding<sup>a</sup>, Ge Ji<sup>b</sup>, Yue Ma<sup>a</sup>, Pengfei Xiao<sup>b</sup>, Li Lu<sup>b</sup>, Jim Yang Lee<sup>a,\*</sup>

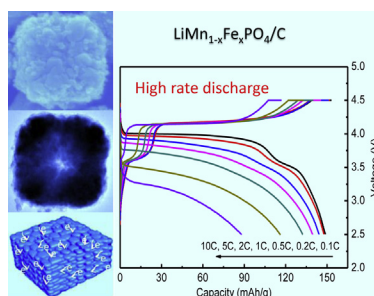
<sup>a</sup> NUS Graduate School for Integrative Sciences and Engineering (NGS), Center for Life Sciences (CeLS), #05-01 28 Medical Drive, Singapore 117456, Singapore

<sup>b</sup> Department of Mechanical Engineering, National University of Singapore, 9 Engineering Drive 1, Singapore 117576, Singapore

## HIGHLIGHTS

- A monodisperse  $\text{LiMn}_{1-x}\text{Fe}_x\text{PO}_4/\text{C}$  cathode with bi-continuous networks for electron and  $\text{Li}^+$  transport.
- Aliovalent doping, carbon coating and mesoscale assembly were used in tandem to optimize performance.
- Excellent electrochemical performance for reversible  $\text{Li}^+$  storage ( $116 \text{ mAh g}^{-1}$  at 5 C,  $88 \text{ mAh g}^{-1}$  at 10 C).

## GRAPHICAL ABSTRACT



## ARTICLE INFO

### Article history:

Received 4 June 2013

Received in revised form

25 August 2013

Accepted 27 August 2013

Available online 5 September 2013

### Keywords:

Bi-continuous

Cathode

High rate

Monodisperse

Phospho-olivine

## ABSTRACT

The performance of lithium manganese phosphate as a lithium-ion battery cathode material is improved by collective and cooperative strategies including Fe substitution, carbon coating, and the assembly of carbon-coated  $\text{LiMn}_{1-x}\text{Fe}_x\text{PO}_4$  nanocrystals into a highly dense packing of monodisperse microboxes. These strategies are implemented experimentally by a facile and scalable synthesis method. The dense packing allows the conductive carbon coating to be interconnected into a continuous three-dimensional network for electron conduction. The porosity in the packed structure forms the complementary network for  $\text{Li}^+$  transport in the electrolyte. The primary particles are nanosized and Fe-substituted to improve the effectiveness of  $\text{Li}^+$  insertion and extraction reactions in the solid phase. The reduction of transport resistance external and internal to the nanocrystals yields a Li storage host with good rate performance ( $116 \text{ mAh g}^{-1}$  at 5 C discharge rate where  $C = 170 \text{ mA g}^{-1}$ ) and cycle stability (95% retention of initial capacity in 50 cycles). Electrochemical impedance spectroscopy and morphology examination of the cycled microboxes reveal a robust packed structure with stable surfaces.

© 2013 Elsevier B.V. All rights reserved.

## 1. Introduction

The relentless efforts in using particle size reduction, conductive surface coating, and mesoscale assembly to improve the

performance of  $\text{LiFePO}_4$  have resulted in a material very different from when it was first introduced [1–6].  $\text{LiFePO}_4$  is now considered as a safe cathode material with good cycle life and reasonable cost for large format lithium ion batteries [2,3,7,8]. Isostructural with  $\text{LiFePO}_4$ ,  $\text{LiMnPO}_4$  offers 20% more energy density because of a voltage plateau which is 0.7 V higher than that of  $\text{LiFePO}_4$  [9]. Similar to the early days of  $\text{LiFePO}_4$ , the development of  $\text{LiMnPO}_4$  is impeded by its extremely low electronic and ionic conductivities [10,11]. Taking a lesson from  $\text{LiFePO}_4$ , aliovalent doping, crystal size reduction, and carbon painting have been applied to  $\text{LiMnPO}_4$  to

\* Corresponding author. Department of Chemical and Biomolecular Engineering, National University of Singapore, 10 Kent Ridge Crescent, Singapore 119260, Singapore. Tel.: +65 6516 2899; fax: +65 67791936.

E-mail address: [cheleejy@nus.edu.sg](mailto:cheleejy@nus.edu.sg) (J.Y. Lee).

increase intrinsic electronic conductivity, shorten the  $\text{Li}^+$  diffusion path length in the nanocrystal, and reduce the external electrical resistance respectively. Success has thus far been limited. The highly insulating nature of  $\text{LiMnPO}_4$ , and the Jahn–Teller distortion of  $\text{Mn}^{3+}$  ions where the mismatch between  $\text{LiMnPO}_4$  and  $\text{MnPO}_4$  phases repel  $\text{Li}^+$  diffusion, [12] thereby requiring more extreme nanocrystal size reduction (to 10 nm and below) to ameliorate the transport limitations in the solid phase. A large amount of carbon is also required for encapsulating the nanocrystal surface when sub-10 nm nanocrystals are used [13]. The use of small nanocrystals and excess carbon would however lower the overall energy density of the cathode material substantially [14].

Recent studies have shown that the partial substitution of Mn with Fe can form  $\text{LiMn}_{1-x}\text{Fe}_x\text{PO}_4$  ( $x$  from 0 to 1) solid solutions with higher electronic and ionic conductivities and less Jahn–Teller distortion [12,15–18], allowing the same level of performance in nanocrystals larger than those of  $\text{LiMnPO}_4$  (sub-100 vs sub-10 nm) [16,19]. Good rate performance in practice, however, still uses an excessive amount of carbon for the electrical connection of discrete nanocrystals. Overall energy density and power density of the cathode therefore remain to be low. The assembly of discrete primary nanocrystals into compact organized aggregates offers an opportunity to improve the volumetric energy and power densities while keeping the nanocrystal advantage [20,21]. The assembly has to be implemented in such a way that it possesses co-continuous electronic and ionic conductive networks for the transport of electrons and  $\text{Li}^+$  [22–24]. Since electron transport between the particles in the aggregates depends on in-situ formed thin carbon films where electrical conductivity may be limited, the aggregate size has to be moderate so as not to incur transport limitations at the aggregate level [25]. Thus mesoscale assembly is preferred over macroscale assembly. Due to the difficulty in synthesizing uniformly sized  $\text{LiMn}_{1-x}\text{Fe}_x\text{PO}_4$  nanocrystals, and the assembly of nanocrystals into mesoscale structures, there have been very few reports on assembled  $\text{LiMn}_{1-x}\text{Fe}_x\text{PO}_4$  structures in the literature. Hence the development of facile and scalable methods for the synthesis and assembly of  $\text{LiMn}_{1-x}\text{Fe}_x\text{PO}_4$  nanocrystals into compact mesoscale structures with co-continuous networks for electron and ion conduction is essential for realizing the true potential of  $\text{LiMnPO}_4$ -based cathodes.

This is a report of design of co-continuous phase-pure monodisperse  $\text{LiMn}_{1-x}\text{Fe}_x\text{PO}_4/\text{C}$  microboxes through collective and cooperative strategies and their preparation. The microboxes were constituted from densely packed carbon-coated 100–200 nm  $\text{LiMn}_{1-x}\text{Fe}_x\text{PO}_4$  nanocrystals. Pores were formed by the interstices in the packed structure. A small amount of Fe substitution was used to improve the intrinsic electrochemical properties of  $\text{LiMnPO}_4$  [26]. Each nanocrystal was coated with a layer of carbon to reduce the electrical resistance between the nanocrystals. The nanocrystals in the microboxes were densely packed so that the carbon coating formed a continuous 3D network for electron conduction through the aggregates. The interstices in the microboxes formed the complementary network of interconnected pores to support efficient electrolyte infusion to reduce the  $\text{Li}^+$  diffusion resistance external to the nanocrystals. Monodispersity of the microboxes also enabled a more even charge distribution and minimized the local perturbations of mass transfer processes. Consequently these monodisperse microboxes were capable of delivering excellent discharge capacities of  $116 \text{ mAh g}^{-1}$  at the 5 C rate ( $C = 170 \text{ mA g}^{-1}$ ) and  $88 \text{ mAh g}^{-1}$  at the 10 C rate. Such impressive rate performance places these microboxes the best of  $\text{LiMnPO}_4$ -based cathodes with low carbon loading. The preparation leveraged firstly on a high yield synthesis of monodisperse  $\text{Mn}_{1-x}\text{Fe}_x\text{PO}_4 \cdot \text{H}_2\text{O}$  microboxes (>95% yield) by probe sonication assisted precipitation. A solution chemistry method that preserved the size and shape of the

microboxes was then applied to implant the carbon source; followed by a finishing heat treatment.

## 2. Experimental section

### 2.1. Materials preparation

The synthesis of monodisperse  $\text{LiMn}_{1-x}\text{Fe}_x\text{PO}_4/\text{C}$  microboxes was a two-step process. Monodisperse  $\text{Mn}_{1-x}\text{Fe}_x\text{PO}_4 \cdot \text{H}_2\text{O}$  microboxes were fabricated first; followed by reactions with lithium acetate and glucose monohydrate in ethanol and heat treatment.

Monodisperse  $\text{Mn}_{1-x}\text{Fe}_x\text{PO}_4 \cdot \text{H}_2\text{O}$  microboxes were prepared by the co-precipitation method. 4.25 g  $\text{Mn}(\text{NO}_3)_2 \cdot 4\text{H}_2\text{O}$  (Sigma Aldrich) and 1.07 g  $\text{Fe}(\text{NO}_3)_3 \cdot 9\text{H}_2\text{O}$  (Sigma Aldrich) were dissolved in ethanol to a total volume of 30 ml, 5 ml  $\text{H}_3\text{PO}_4$  (85 wt.%) (Malinckrodt) was then added quickly under probe sonication (Sonics VCX 750 W) for 1 min. The resultant solution was transferred to a 50 ml Teflon-lined autoclave for 1 h of reaction at  $40^\circ\text{C}$ . The reaction product was recovered as a precipitate, washed twice with DI water and centrifuged, and dried at  $60^\circ\text{C}$  for 12 h. The progress in microbox formation was sampled by analysing the reaction mixture at 15 min, 30 min, 40 min, 1 h and 4 h into the reaction.

The synthesis of  $\text{LiMn}_{1-x}\text{Fe}_x\text{PO}_4/\text{C}$  was then carried out as follows: equimolar quantities of  $\text{LiCH}_3\text{COO} \cdot 2\text{H}_2\text{O}$  (Sigma Aldrich) and  $\text{Mn}_{1-x}\text{Fe}_x\text{PO}_4 \cdot \text{H}_2\text{O}$ ; and 30 wt.% glucose monohydrate were mixed in ethanol and bath-sonicated for 1 h (Branson 2510). Ethanol was then allowed to evaporate and the residue was calcined at  $600^\circ\text{C}$  in flowing Ar for 12 h in a tube furnace. For comparison a sample, SSR-nano was also prepared by the solid-state reaction from a mixture of  $\text{LiCH}_3\text{COO} \cdot 2\text{H}_2\text{O}$ ,  $\text{Fe}_2\text{O}_3 \cdot 2\text{H}_2\text{O}$  (Sigma Aldrich),  $\text{Mn}(\text{CH}_3\text{COO})_2 \cdot 4\text{H}_2\text{O}$ ,  $\text{NH}_4\text{H}_2\text{PO}_4$  (Sigma Aldrich) (Li:Fe:Mn:P = 1:0.13:0.87:1) and Super P carbon (10 wt.% of the final product). The mixture was ball-milled intermittently for a total of 4 h (30 min grinding followed by 30 min of rest). The mixture was heat-treated at  $350^\circ\text{C}$  for 10 h, mixed with 10 wt.% sucrose and ball-milled again for one more hour before another heat-treatment at  $600^\circ\text{C}$  for 12 h in flowing Ar.

### 2.2. Materials characterization

The morphologies of  $\text{LiMn}_{1-x}\text{Fe}_x\text{PO}_4/\text{C}$  microboxes and SSR-nano were examined by FESEM on a JEOL JSM-6700F; and by FETEM on a JEOL JEM-2010F. The carbon content in  $\text{LiMn}_{1-x}\text{Fe}_x\text{PO}_4/\text{C}$  was assayed by TGA on a Shimadzu DT-60H. Crystal structure determinations were based on X-ray diffraction measurements of the samples on a Bruker D8 Advance diffractometer using  $\text{Cu K}\alpha$  irradiation. EDX measurements were performed during the FESEM and FETEM sessions to obtain average elemental compositions and the compositions of single microboxes respectively.

### 2.3. Electrochemical measurements

Monodisperse  $\text{LiMn}_{1-x}\text{Fe}_x\text{PO}_4/\text{C}$  microboxes or SSR-nano ( $\sim 50 \text{ nm}$ ), Super P carbon and polyvinylidene fluoride (PVDF) (Sigma Aldrich) in a weight ratio of 8:1:1 were mixed into a consistent slurry in *N*-methylpyrrolidone (NMP) (Sigma Aldrich). The slurry was applied uniformly on an aluminium foil current collector to a loading of  $\sim 3 \text{ mg cm}^{-2}$  followed by drying in vacuum at  $120^\circ\text{C}$  overnight. The thickness of the finished electrodes (after compression at 2 ton pressure) was  $12 \mu\text{m}$  for the microboxes and  $20 \mu\text{m}$  for SSR-nano. Electrode density, on the other hand, was  $2.5 \text{ g cm}^{-3}$  for the former and  $1.5 \text{ g cm}^{-3}$  for the latter. The difference in electrode thickness was due to the difference in material packing density. The working electrode, a lithium foil counter *cum* reference electrode, and a Celgard 2400 membrane separator were

Download English Version:

<https://daneshyari.com/en/article/7738989>

Download Persian Version:

<https://daneshyari.com/article/7738989>

[Daneshyari.com](https://daneshyari.com)